

Department of Pulmonary Diseases<sup>1</sup>, Heilongjiang Academy of Chinese Medicine Science; Department of Respiratory Medicine<sup>2</sup>, Fourth Affiliated Hospital, Harbin Medical University Harbin, Heilongjiang, China

## TIM-1 attenuates airway mucus hypersecretion and inflammation induced by cigarette smoke via the PI3K/Akt signaling pathway

QIANG LI<sup>1, #</sup>, HANG SHANG<sup>2, #</sup>, XIANGSHUN LI<sup>2</sup>, GUANGRUN WU<sup>2</sup>, LIXIA QIANG<sup>2, \*</sup>

Received September 2, 2024, accepted October 8, 2024

\*Corresponding author: Lixia Qiang, Department of Respiratory Medicine, Fourth Affiliated Hospital, Harbin Medical University, 37# Yiyuan Street, Harbin, Heilongjiang, China, 150001  
qianglixia2012@hrbmu.edu.cn

<sup>#</sup>These authors contributed equally to this work.

Pharmazie 79: 220-227 (2024)

doi: 10.1691/ph.2024.4612

Pharmazie is a full open access journal following the CC BY 4.0 license model.

Cigarette smoke extract (CSE)-induced airway mucus hypersecretion and inflammation are prominent features of chronic obstructive pulmonary disease (COPD). As a factor associated with inflammation regulation, T cell immunoglobulin and mucin domain-1 (TIM-1) is found to be involved in various inflammatory disorders such as asthma and COPD. In this study, the GEO database provides two human COPD gene expression datasets (GSE67472, n = 62) along with the relevant controls (n = 43) for differentially expressed gene (DEG) analyses. Candidate biomarkers are identified, and the discriminatory ability is determined using the area under the receiver operating characteristic curve (AUC) values. Furthermore, a COPD mouse model is established using CSE to validate that anti-TIM-1 can attenuate airway mucus hypersecretion and inflammation via the PI3K/Akt signaling pathway in COPD. Anti-TIM-1 antibody pretreatment significantly suppresses mucin secretion, inflammatory cell infiltration, and inflammatory cytokine release in mouse lungs induced by CSE and also suppresses CSE-induced expression of MUC5AC. Western blot shows that the anti-TIM-1 antibody attenuates the activation of p-Akt in airway mucus hypersecretion mice induced by CSE. This study highlights the protective effect of the TIM-1 antibody on CSE-related airway mucus hypersecretion and inflammation, in which PI3K/AKT may be involved. These findings suggest that TIM-1 could be a potential therapeutic target for airway mucus hypersecretion.

### 1. Introduction

Chronic obstructive pulmonary disease (COPD) is a complex and multifactorial disease caused by a combination of environmental and genetic factors (Agustí et al. 2022). Cigarette smoking is considered to be the main risk factor of COPD in Western countries and China (Mannino and Buist 2007; Wang et al. 2018). It has been reported that cigarette smoking-induced abnormal inflammatory responses contributes to COPD (Mannino and Buist 2007). Cigarette smoke can impair mucociliary transport by inducing airway dehydration and increasing mucus viscosity, leading to further deterioration of lung condition in smokers with COPD (Pauwels et al. 2011; Yang et al. 2023). As a worldwide health problem, airway mucus hypersecretion is a vital pathophysiologic feature in COPD patients, which contributes to the irreversible airflow limitation in COPD (Agustí et al. 2022; Sharma et al. 2023; Yang et al. 2023). It not only affects the quality of life of patients, but also poses a continuous threat to their life expectancy (Agustí et al. 2022). So, it is key to strategizing in the management of COPD. Therefore, attenuating airway inflammatory response and mucin secretion has been identified as an effective approach to the therapy of COPD (Sharma et al. 2023; Yang et al. 2023).

T cell immunoglobulin domain, mucin-like domain-1 (TIM-1) is a member of the TIM family of genes and encodes transmembrane glycoprotein proteins expressed by CD4 T cells (de Souza et al. 2005; Mariat et al. 2009; Yeung et al. 2015). TIM-1 was founded to a critical gene that regulates T-helper cell development and Th2 airway inflammation in bronchial asthma and allergic rhinitis (Curtiss et al. 2012). It was reported that TIM-1 gene polymorphisms

was associated with allergic rhinitis susceptibility in a Han Chinese population, Korean population and childhood asthma (Chae et al. 2005; Li et al. 2011; Chen et al. 2012). In addition, the exposure of phosphatidylserine (PtdSer) on apoptotic cells activates TIM-1, which induces asthma. Fine particulate matter (PM<sub>2.5</sub>) exacerbates airway inflammation and AHR in asthmatics (Yang et al. 2020). Moreover, PM<sub>2.5</sub>-induced exacerbation of AHR associated with allergic asthma was associated with increased apoptosis and TIM-1 activation (Yang et al. 2020). Several research groups have determined the function of TIM-1 in Th2-associated diseases by targeting TIM-1 through recombinant mouse TIM-1 monoclonal antibodies (mAbs) (Xiao et al. 2015; Hosseini et al. 2018). In mouse models of asthma, intranasal administration of anti-TIM1 have been shown to ameliorated allergic lung inflammation and reduce Th2 cytokine production (Fukushima et al. 2007). The relationship between TIM-1 and asthma implies that targeting TIM-1 with recombinant anti-TIM-1 mAbs may reduce mucous cell metaplasia in COPD.

In this study, we used R-packet CIBERSORT to analyze immune cell differences in patients with airway mucus hypersecretion. Differential gene analysis was performed by limma package to screen out the differential genes between patients with airway mucus hypersecretion and normal controls. Then, we explored the role of TIM-1 in CSE exposure-induced mucus hypersecretion and airway inflammation in vivo, and we found that TIM-1 antibody dramatically suppressed CSE-induced inflammatory response and mucus hypersecretion possibly through downregulating the activation of PI3K/Akt signaling pathways. The result of this study provides a new potential target for COPD prevention and treatment.

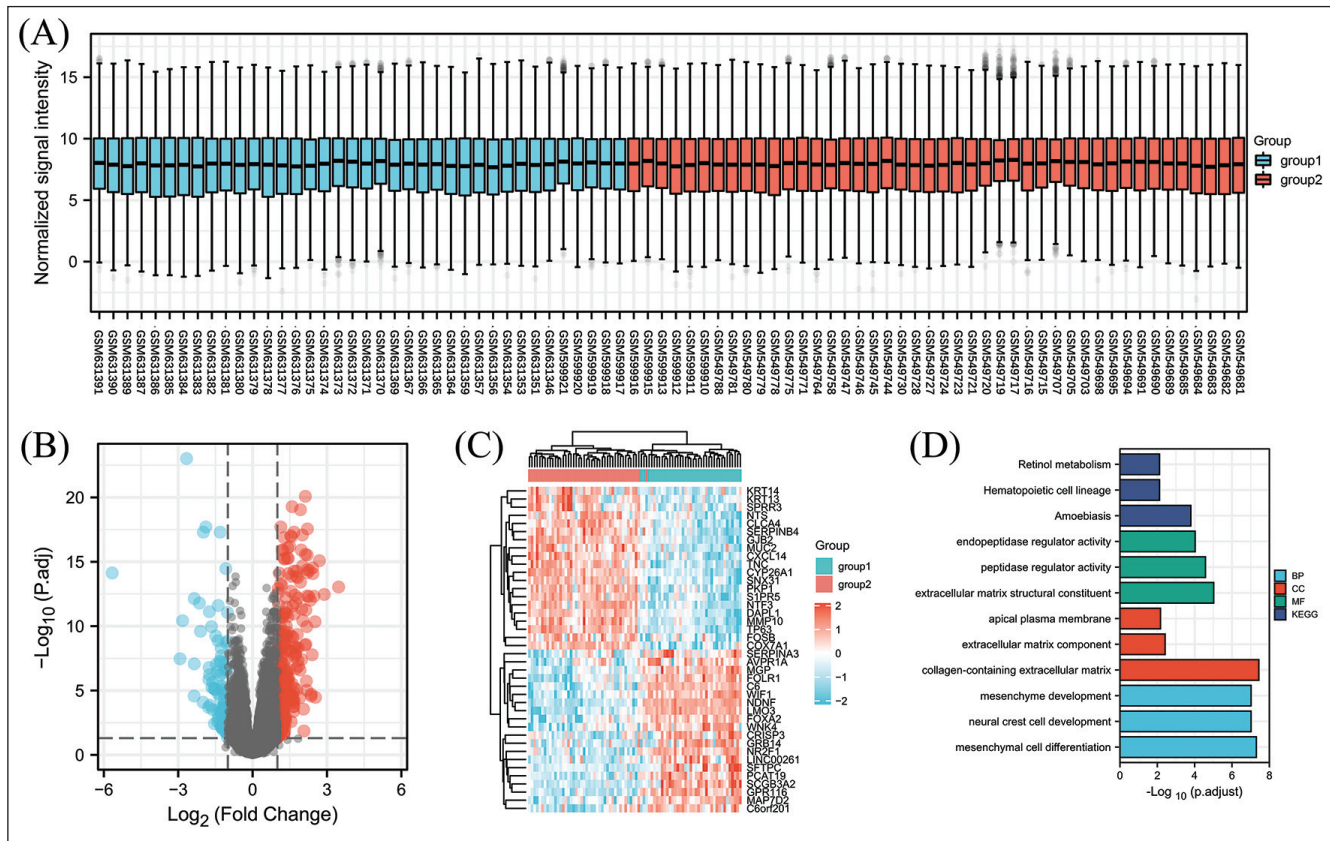


Fig. 1: Differentially expressed genes (DEGs) between airway mucus hypersecretion tissues and normal samples in metadata ((GSE67472 dataset) cohort). (A) Data graph after batch correction; (B) Volcano plot of DEGs; (C) Heatmap plot of DEGs; (D) Enrichment analysis of DEGs.

2. Investigations and results

2.1. Screening of DEGs in COPD

Differential expression analysis between 62 airway mucus hypersecretion samples and 49 normal samples in the metadata (GSE67472) cohort was carried out utilizing the “limma” R package. The data diagram after batch correction is shown in Figure 1 A. Of the 398 identified DEGs, 290 genes were significantly upregulated and 108 genes were significantly downregulated (Fig. 1B, 1C). As shown in Fig. 1D, differential gene enrichment analysis showed that most of the enrichment pathways were related to immune cell infiltration.

2.2. Immune cell infiltration landscape

With the CIBERSORT algorithm, we firstly calculated the proportion of immune cell infiltration in airway mucus hypersecretion and normal tissues. The results showed that the degree of infiltration of resting plasma cells (P = 0.05), T cells CD8 (P = 0.01), T cells CD4 memory activated (P = 0.001) and T cells follicular (P = 0.001) in airway mucus hypersecretion tissues were notably raised in contrast to controls. Conversely, control samples demonstrated a higher proportion of infiltration of M2 macrophages (P=0.001) and dendritic cells activated (P=0.05) compared to those found in airway mucus hypersecretion tissues (Fig. 2A). The heatmap of each immune cell is depicted in Figure 2B. Figure 2C shows the difference in immune cells between the healthy and diseased groups, suggesting that T lymphocytes, macrophages, and mast cells are the main differentiating immune cells.

2.3. WGCNA and functional enrichment analysis of DEGs

A gene co-expression network was constructed using R package “WGCNA” and cluster analysis was performed on 106 samples. To construct the scale-free network, we chose  $\beta=4$  (scale-free  $R^2=0.85$ ) as the soft threshold power (see Fig. 3A). A hierarchical clustering tree was constructed using dynamic hybrid cutting tech-

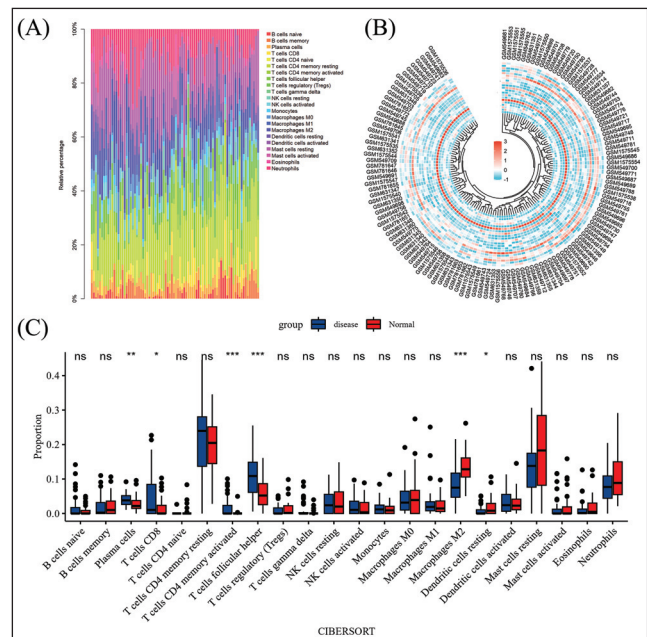


Fig. 2: Landscape of immune cell infiltration in airway mucus hypersecretion. (A) Histogram of immune cell infiltration; (B) A heatmap of each sample of immune cells; (C) Boxplot of the proportion of 22 types of immune cell infiltrates. \* p<0.05 indicates significant differences. \*\*P < 0.01 indicates extremely significant differences. ns, not significant differences.

niques, where each leaf represents a sample and genes with similar expression data are clustered together to form a branch of the tree, which represents gene modules (Fig. 3B). Figure 3C shows that genes are assigned into modules of different colors. The heat map

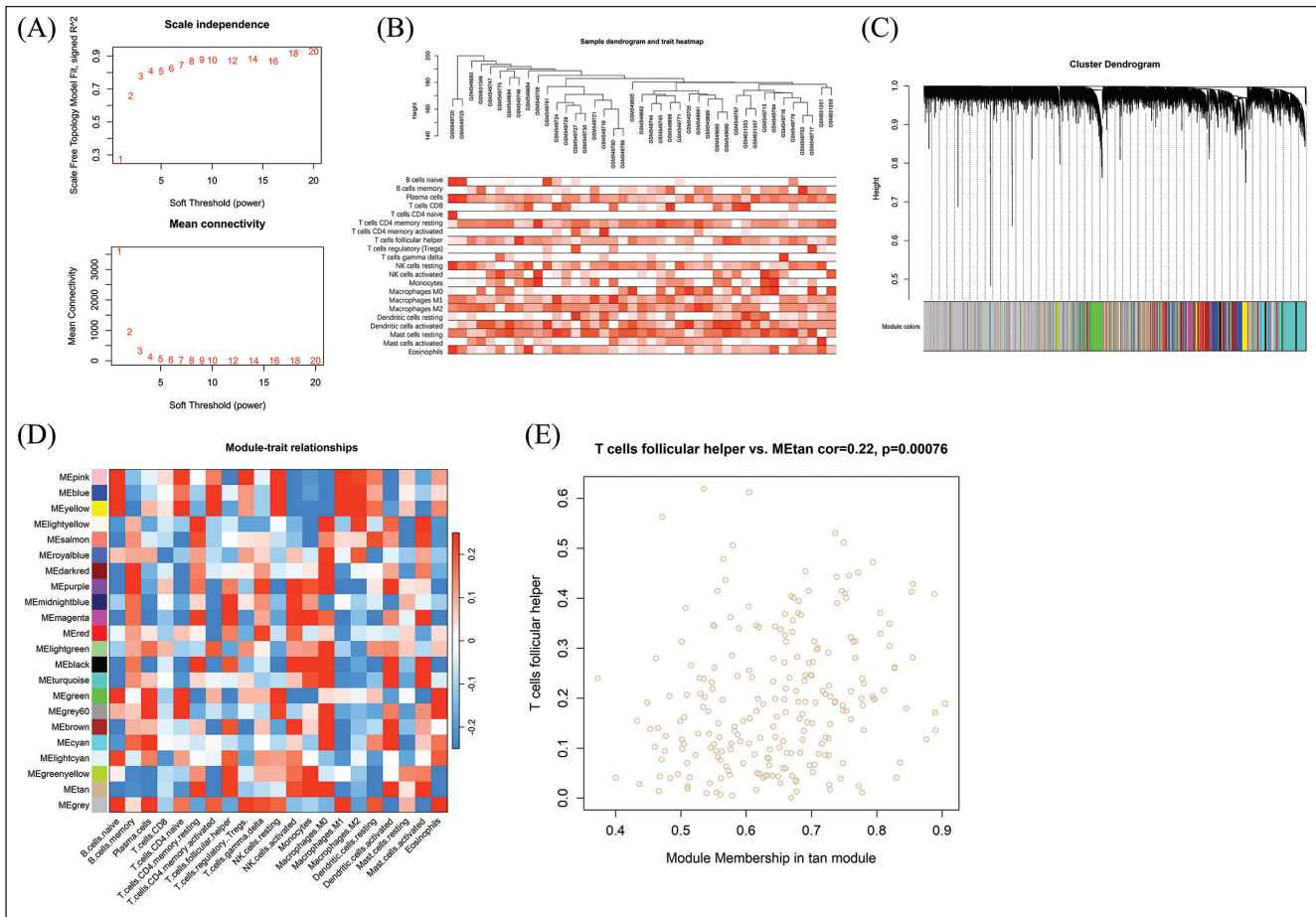


Fig. 3: Gene co-expression network and cluster analysis. (A) Soft threshold power. (B) Gene module. (C) Genes are assigned to modules of different colors. (D) Heat map of correlation between different modules and immune cells. Red indicates a positive correlation and blue indicates a negative correlation. (E) Key gene of METAN module.

of the correlation between different modules and immune cells showed that red indicates positive correlation and blue indicates negative correlation (Fig. 3D). We found that the changes of T cells were particularly significant, so we screened the modules related to T cells, and finally found that METAN module had the highest correlation with T cells, and we found TIM1 as the key gene of METAN module (Fig. 3E).

**2.4. Screen hub gene with PPI network**

PPI network was constructed for key WGCNA module genes, and then the first five algorithms of cytoHubba plug-in of Cytoscape (v 3.7.2) were used to score each node gene. Finally, two key genes (TIM1 and P13K) were screened using “UpSet”(Fig. 4).

**2.5. Anti-TIM-1 alleviates mouse lung histologic changes induced by CSE**

To evaluate the histologic changes following CSE exposure and anti-TIM1 body pretreatment, H&E staining was performed based on the fixed mouse lungs. The slices showed that four-week CS exposure dramatically increased airway epithelium thickening, airway epithelial cell hyperplasia, peribronchial inflammatory cell infiltration, and lumen obstruction by mucus and cell debris. However, all these changes were alleviated by anti-TIM1 body pretreatment (Figure 5A and B).

**2.6. Anti-TIM-1 suppresses the mucus hypersecretion induced by CSE in mouse lungs**

AB-PAS staining showed that CSE exposure highly increased the secretion of airway mucus proteins which were stained as blue, and anti-TIM-1 body pretreatment suppressed the expression of

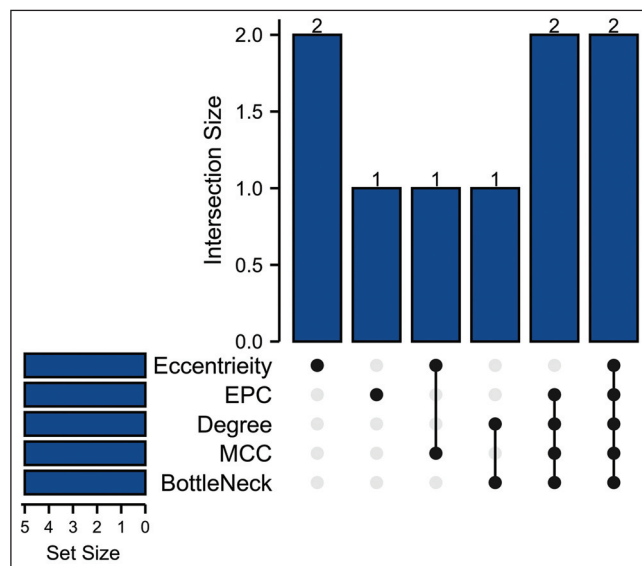


Fig. 4: Construct PPI network and screen hub gene.

mucins in mouse airways (Fig. 6A and B). As the major source of airway mucus, the expression level of MUC5AC was detected with qRT-PCR and western blot. The results showed that after 4-week CSE exposure, both the mRNA and protein levels of MUC5AC in mouse lungs were dramatically increased, and the elevated MUC5AC mRNA and proteins were attenuated by anti-TIM-1 body treatment (Fig. 6C, D and E).

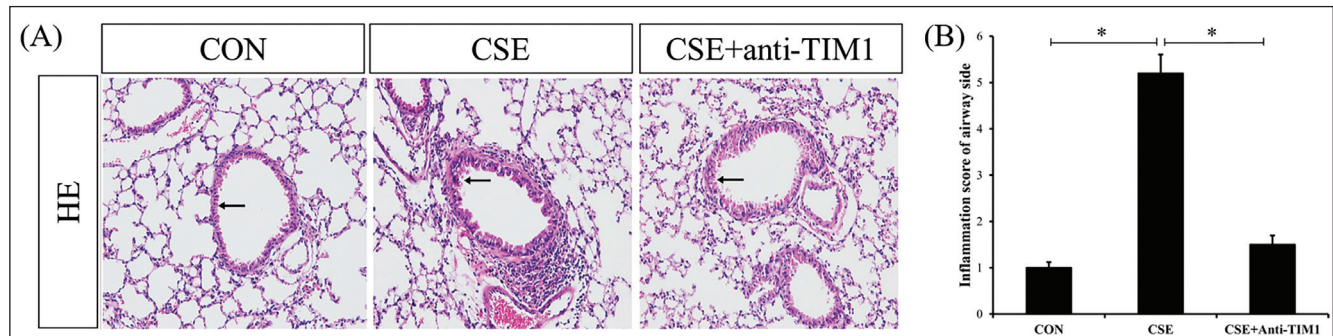


Fig. 5: Effect of anti-TIM1 on airway inflammation in CSE-induced mucus hypersecretion in the mice model of COPD. (A) Representative photomicrographs of HE staining lung sections (magnification,  $\times 200$ ). (B) Inflammation score of the airway and airway side in mice of each group. Graphs display a summary of two to three independent experiments. Data are expressed as the mean  $\pm$  SEM. \*  $p < 0.05$  indicates significant differences.

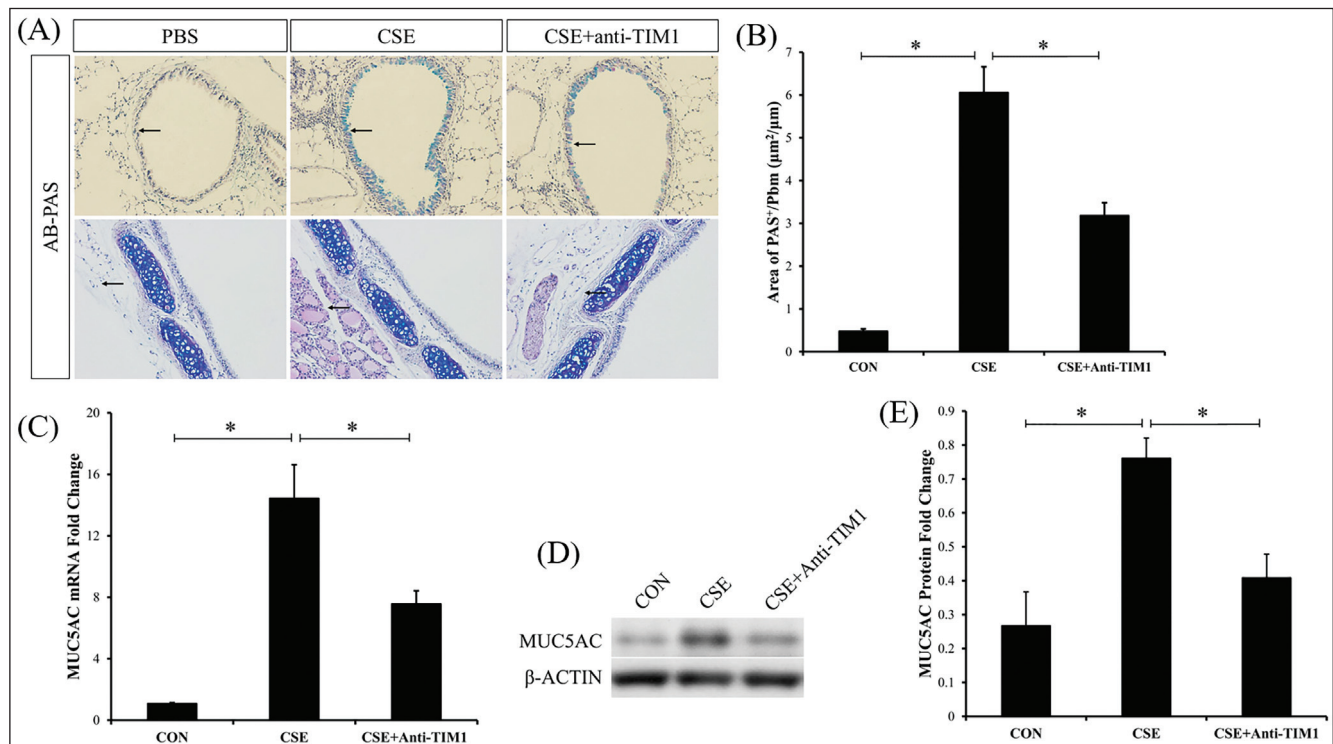


Fig. 6: Intranasal administration of Anti-TIM1 prevents CSE-induced mucus hypersecretion in the mice model of COPD. (A) Representative photomicrographs of PAS-stained lung sections (magnification,  $\times 100$ ). (B) The PAS positive area per total area was measured. (C) The expression of MUC5AC mRNA in mouse lung tissues was evaluated by RT-qPCR. (D) The expression of MUC5AC mRNA in mouse lung tissues was evaluated by western blot. Corresponding densitometric analyses of the protein bands of (E) MUC5AC/ $\beta$ -actin. Graphs display a summary of two to three independent experiments. Data are expressed as the mean  $\pm$  SEM. Anti-TIM1, Tim1 antibody; CSE, cigarette smoke extract; PAS, periodic-acid Schiff; Pbm, perimeter of basement membrane. \*  $p < 0.05$  indicates significant differences.

### 2.7. Anti-TIM-1 decreases CS-induced inflammatory cell release in mouse BALF

The total cell number from BALF samples in the PBS group was significantly lower compared with the mice of CSE group (Fig. 7A). And the total cell number in CSE+Anti-TIM1 group significantly decreased compared with the CSE group (Fig. 7B). In the CSE +Anti-TIM1 group, the numbers of different inflammatory cells from BALF, including macrophagocytes, lymphocytes and eosinophils, were also significantly reduced compared with the CSE group (Fig. 7C).

### 2.8. Anti-TIM1 down-regulates CSE-induced increase of IL-1 $\beta$ , IL-6 and TNF- $\alpha$ in BALF and serum

To determine whether anti-TIM1 ameliorates inflammation and altered cytokine profiles, the concentration levels of the latter markers, IL-6, IL-1 $\beta$  and TNF- $\alpha$  were examined in both BALF and serum samples derived from mice. The CSE group exhibited significantly higher levels of IL-6, IL-1 $\beta$  and TNF- $\alpha$  were

observed compared with in the PBS group (Figure 8). Compared with the CSE group, intranasal administration of anti-TIM1 led to a significant reduction of IL-6, IL-1 $\beta$  and TNF- $\alpha$  (Fig. 8).

### 2.9. TIM1 activates the PI3K/Akt pathway in mice

The protein levels of Akt and p-Akt were detected in lung tissues using western blot. Compared with PBS group, the protein expression levels of p-Akt was significantly upregulated in the CSE group, whereas these were reduced in the CSE+Anti-TIM1 group compared with the CSE group (Fig. 9).

## 3. Discussion

Chronic airway inflammation induced by cigarette smoke (CS) has been recognized as one of the major characteristics of COPD. It has been demonstrated that the levels of inflammatory cytokines and chemokines in BALF and circulation among COPD smokers were significantly higher than those in non-smoker COPD patients or non-smoker healthy individuals (Barnes 2016). Moreover, CS

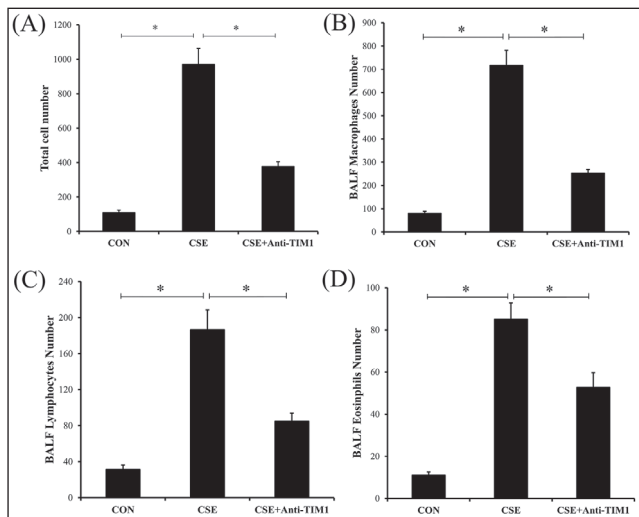


Fig. 7: Intranasal administration of Anti-TIM1 alleviates airway inflammation in the mice model of COPD. (A) The total cell number in the BALF samples. The macrophagocytes(B), lymphocytes(C) and eosinophils(D) cell number in the BALF samples. Graphs display a summary of three independent experiments. Data are expressed as the mean  $\pm$  SEM. BALF, bronchoalveolar lavage fluid; Anti-TIM1, Tim1 antibody; CSE, cigarette smoke extract. \* $p < 0.05$  indicates significant differences.

exposure remarkably activated airway inflammatory responses both in vivo and in vitro (Kistemaker et al. 2013; Wang et al. 2016). In this study, we presented novel evidence that anti-TIM1 played protective roles in CS-induced airway inflammation, suggesting the therapeutic potential of anti-TIM1 in CS-related pulmonary inflammatory disorders such as COPD.

Weighted gene co-expression network analysis (WGCNA) can offer in-depth insights into gene networks, hub genes, and the pathogenesis related to asthma (Wang et al. 2023). In this research, we hypothesized that evaluating gene expression in airway epithelial cells through WGCNA might identify the gene-network signature, provide potential biomarkers for T2-high asthma, and further predict treatment responses. TIM-1 was identified as being significantly correlated with asthma status (McIntire et al. 2004; Mariat et al. 2009). The turquoise module observed in this study was positively correlated with asthma traits and considered as the most crucial module in the pathogenesis of T2-high asthma. This implies that the TIM-1 gene likely participates in the pathogenesis and immune imbalance and could serve as a potential biomarker for the diagnosis and a therapeutic target of T2-high asthma.

TIM-1 has been recognized as a crucial susceptibility gene for asthma (Xie et al. 2017; Niu et al. 2018). Previous studies have found that the inhibition of TIM-1 signaling can downregulate the level of T cell infiltration into allergic skin tissues and tissues related to autoimmune diseases (Brunton et al. 2019). In a prior study, it was found that injecting intraperitoneal anti-TIM-1 antibodies into a mouse model of allergen-induced asthma reduced the level of Th2 cytokines and inhibited inflammatory cell infiltration in the airway (Fukushima et al. 2007). Airway hyperresponsiveness (AHR) is one of the key characteristics of asthma and a major factor contributing to the pathogenesis of this disease (O'Byrne and Inman 2003). AHR is characterized by increased airway resistance and decreased airway compliance (Kaczka et al. 1999). The results of the present study demonstrated that intranasal administration of Anti-TIM1 could reduce the number of inflammatory cells in BALF and serum samples and reverse methacholine-induced AHR. This indicated that Anti-TIM1 can effectively attenuate airway inflammation and AHR in experimental asthma, which is in line with previous studies showing that anti-TIM-1 modulates TIM-1 activity in response to allergen challenge in CS-induced chronic airway inflammation (Hosseini et al. 2018).

Apart from chronic inflammation, excessive secretion of airway mucus also contributes to the initiation and progression of COPD. Chronic exposure to cigarette smoke (CS) has been identified as

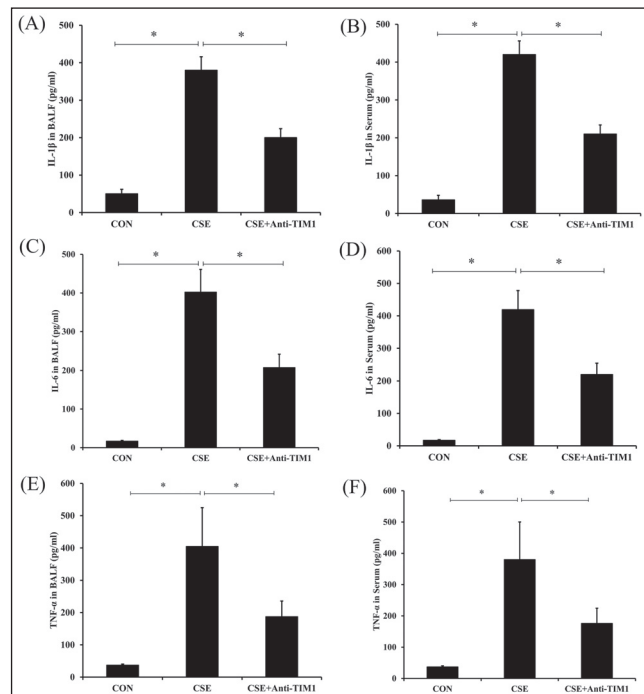


Fig. 8: The concentration levels of IL-1 $\beta$ , IL-6 and TNF- $\alpha$  in serum and BALF samples were measured by ELISA. The concentration levels of IL-1 $\beta$ (A), IL-6(C) and TNF- $\alpha$ (E) in BALF. The concentration levels of IL-1 $\beta$ (B), IL-6(D) and TNF- $\alpha$ (F) in serum. The data are expressed as the mean  $\pm$  standard error of the mean of three independent experiments. IL, interleukin; BALF, bronchoalveolar lavage fluid; Anti-TIM1, Tim1 antibody; CSE, cigarette smoke extract; TNF, tumor necrosis factor. \* $p < 0.05$  indicates significant differences.

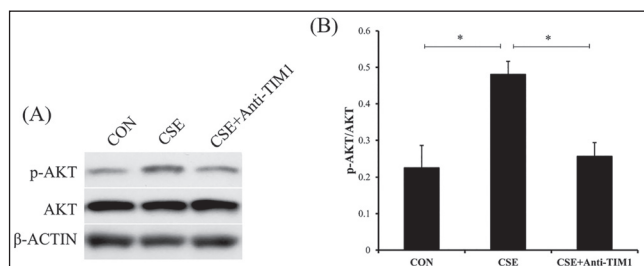


Fig. 9: Western blot analysis of the protein expression levels of p-Akt and Akt in mouse lung tissues (A) Western blots of p-Akt and Akt in mouse lung tissues. Corresponding densitometric analyses of the protein bands of (B)p-Akt/Akt. Graphs display a summary of three independent experiments. Data are expressed as the mean  $\pm$  SEM. p, phosphorylated. \* $p < 0.05$  indicates significant differences.

the most common trigger for mucin secretion (Barnes 2017; Agustí et al. 2022). Additionally, a deficiency in TIM-1 has been demonstrated to reduce the occurrence of allergic asthma in a mouse model (Kim et al. 2013). It has also been reported that agonistic TIM-1 monoclonal antibodies (clone 3B3 and clone 1H8.2) enhance T cell-mediated immune responses, while an antagonistic antibody inhibits the immune response through regulatory B cells (Ding et al. 2011). In this study, the results of H&E and AB-PAS staining indicate that the CSE+Anti-TIM1 group treated with anti-TIM-1 shows a significant reduction in mucous cells in the bronchial epithelium. The mRNA expression of MUC5B is significantly downregulated in the CSE+Anti-TIM1 group compared to that in the CSE group. Understanding the functions of TIM-1 in contributing to asthma susceptibility and severity is of great significance for both asthma treatment and prevention.

Cigarette smoking-induced abnormal inflammatory responses contributes to COPD (Barnes 2016; Sharma et al. 2023). Cigarette smoke can cause inflammation and induce apoptosis of alveolar epithelial cells via release of TNF- $\alpha$  (Guan et al. 2020). IL-1 $\beta$  is

found to be induced in cigarette smoke extract (CSE)-induced airway epithelial cells (Dang et al. 2020). Neutrophilic inflammation mediated by IL-1 $\alpha$  is observed to be augmented in COPD patients (Pauwels et al. 2011). Macrophages within the lungs can produce IL-8/CXCLs, resulting in an increased inflammatory response by inducing leukocytes from the circulatory system to the inflammatory site (Wu et al. 2018). Additionally, other pro-inflammatory cytokines (IL-1 $\beta$  and IL-6) are also proven to be crucial mediators in CSE-induced lung inflammation in COPD (Kersul et al. 2011). TIM-1 can promote T cell proliferation and differentiation by binding to different agonistic ligands (Meyers et al. 2005; Feng et al. 2008). TNF- $\alpha$  has been reported to trigger mucus production in airway epithelium through several intracellular signal transduction cascades, including the EGFR and NF- $\kappa$ B pathways (Busse et al. 2009; Ahmad et al. 2023). TIM-1 molecules bound with agonistic TIM-1 mAbs (Xiao et al. 2007) or other agonistic ligands can produce a strong costimulatory signal for the activation of T cells, thereby promoting T cell differentiation and proliferation *in vivo*, activating cytokine production, and enhancing the antigen-induced immune response of T cells (Sizing et al. 2007; Schweigert et al. 2014). In a cisplatin-induced acute renal injury model, blocking TIM-1 signaling can significantly reduce the number of CD8 $^{+}$  T cells and inhibit TNF- $\alpha$  secretion, indicating that TIM-1 costimulatory signaling can enhance the effect of CD8 $^{+}$  T cells (Nozaki et al. 2011). Our present study shows that the serum and BALF concentration levels of Th1 cytokines (TNF- $\alpha$ ) and Th2 cytokines (IL-1 $\beta$ , IL-6) are lower in the CSE+Anti-TIM1 group than in the CSE group, suggesting that the decreased production of Th2 cytokines and Th1 cytokines may contribute to the effects of anti-TIM1 on CS-induced chronic airway inflammation in this experimental model.

The PI3K/Akt signaling pathway holds a crucial position in the pathological process of airway remodeling in COPD and asthma (Gutor et al. 2022). It is activated by inflammatory factors such as IL-1 $\beta$ , IL-6, and TGF- $\beta$  (Li et al. 2021). Phosphorylation of Akt is a hallmark of PI3K activation (Revathidevi and Munirajan 2019). The PI3K/Akt pathway is widely involved in a variety of cellular processes including cell differentiation and proliferation, inflammation, metabolism, and apoptosis (Miricescu et al. 2021). In this study, the anti-TIM1 group exhibited lower protein expression of p-Akt. This suggests that anti-TIM1 alleviates airway remodeling, which may be due to enhanced activity of the p-Akt pathway. Nevertheless, a limitation of this study is that the effect of TIM-1 on the PI3K/Akt signaling pathway was not evaluated *in vitro*. Additionally, whether TIM-1 affects the PI3K/Akt signaling pathway in lung structural cells was not assessed.

In summary, TIM-1 was identified as candidate biomarkers of COPD in METAN module. Anti-TIM1 exhibited anti-inflammatory and anti-mucus properties in CS exposure-stimulated mice and airway epithelial cells, and the down-regulating of PI3K/Akt pathways would be involved. Our findings provide new experimental evidence that TIM-1 is a potential candidate for future CS-induced chronic airway inflammation.

## 4. Experimental

### 4.1. Data collection and download

Airway mucus hypersecretion gene expression data collected from the GEO database (<http://www.ncbi.nlm.nih.gov/geo>). GSE67472 dataset was downloaded as a qualified dataset. Inclusion criteria were as follows: (1) Expression profiles of airway mucus hypersecretion and healthy adults were included in the dataset. (2) The data set contains one or more samples.

### 4.2. Data preprocessing and research design

First, download the GSE67472 expression profile data was downloaded. Using R package *affy*, the sample was normalized. Then, the SA packet pair was used to eliminate the batch-like effect. The normalized gene expression matrix was analyzed using the R package “*limma*” package.

### 4.3. Immunoinfiltrate expression analysis

CIBERSORT is a deconvolution algorithm that quantifies immune cell infiltration (22 various cell types) in airway mucus hypersecretion gene expression profiles. The “*corplot*” R package was used to carry out visualization and correlation analysis

of 22 types of infiltrating immune cells including macrophages (M0, M1, and M2), T cells (CD8 $^{+}$  T cells, CD4 $^{+}$  T cells, memory activating CD4 $^{+}$  T cells, Tfh cells, regulatory T cells, and  $\gamma\delta$  T cells), natural killer cells (resting and activated NK cells), mast cells (resting and activated mast cells), B cells (naive B cells and memory B cells), dendritic cells (resting and activated dendritic cells), monocytes, plasma cells, neutrophils and eosinophils. Differences in infiltrating immune cells between airway mucus hypersecretion and healthy samples were visualized using boxplots drawn with the “*ggplot2*” package in R.

### 4.4. Functional enrichment analysis

The R package “*org.Hs.eg.db*” was used to convert gene names into gene ids, and the R package “*clusterProfiler*” was used for gene ontology (GO) and Kyoto Encyclopedia of Genes and Genomes (KEGG) analysis of DEGs. The GO terms and signal pathways with significant differences were screened by threshold values  $p$  value <0.05 and  $q$  value <0.05. The R packages “*enrichment plot*” and “*ggplot2*” were used to visualize the results.

### 4.5. Mouse groups and treatments

In this study, female C57BL/6 mice weighing (18–20) g and aged 6–8 weeks were used. All animals were maintained in a pathogen-free environment at the Animal Center of the Experimental Center of the Fourth Affiliated Hospital of Harbin Medical University (Harbin, China). The mice were housed in a light- and temperature-controlled room with free access to deionized drinking water and standard chow. All experiments were approved by the local animal care committee of the Fourth Affiliated Hospital of Harbin Medical University Center (HRBMUEC20220086).

All mice were randomly divided into three groups, CON group: wild type (WT)+phosphate-buffered saline (PBS), CSE group: WT+CSE (CSE) and CSE+anti-TIM1 group: WT+CSE+anti-TIM1 (CSE+anti-TIM1). The brief steps were as described as follows. The smoke of non-filter cigarette was dissolved in PBS to prepare cigarette smoke extract (CSE). CSE was used to construct the COPD. Mice in each group were weighed and intraperitoneally injected CSE according to their weight (0.3ml/20g). CSE was injected intraperitoneally every 2 weeks for 8 weeks. At the same time, a nasal drip of a certain concentration of CSE is administered every other week. Mice in the control group were injected intraperitoneally or intranasally with sterile PBS by the same method at the same time point. After this procedure, the mice were then observed for abnormal manifestations, such as coughing, agitation, wheezing, or death. Lung tissue and bronchoalveolar lavage fluid (BALF) were collected for further detection.

### 4.6. Cigarette smoke extract preparation

Cigarette smoke extract (CSE) was freshly prepared. Briefly, mainstream smoke from five cigarettes was drawn slowly into a 50 mL syringe and bubbled through 4mL of PBS medium prewarmed at 37 °C. Then this solution, considered to be 100% CSE, was adjusted to pH 7.2–7.4 and sterilized with a 0.22  $\mu$ m filter. Before use, this 100% CSE was diluted with serum free PBS medium to the required CSE concentrations. The extracted CSE was applied to the experimental mice within 30 minutes.

### 4.7. Hematoxylin and eosin (HE) staining

Mouse left lungs without lavage were fixed with 4% phosphate buffered paraformaldehyde under a constant pressure of 25 cm H<sub>2</sub>O. Paraffin embedded lung tissues collected were cut into slices for histological staining. HE staining was performed according to the manufacturer’s instructions (Solarbio, Beijing, China). Briefly, lung tissues from the left lobe were fixed with 4% paraformaldehyde for 24 h and embedded in paraffin. Tissue sections (4  $\mu$ m) were stained with HE to evaluate morphological changes in lungs.

### 4.8. Alcian blue (AB) – Periodic acid-Schiff (PAS) staining

AB-PAS staining was used to observe goblet cell metaplasia and mucus secretion in lungs. All slides were assessed using light microscopy at  $\times 200$  magnification. Bronchioles with a 150–200 $\mu$ m internal diameter were selected in a blinded manner, observed, and photographed. The area of AB-PAS staining was measured using Image-Pro Plus software. The AB-PAS staining area/Pbm ratio was quantified in the airway epithelium.

### 4.9. ELISA assay

Serum and BALF levels of IL-1 $\beta$ , IL-6 and TNF- $\alpha$  were measured with ELISA kits (Wanlei bio, Shanghai, China) according to the manufacturer’s instructions. The absorbance data were measured with a Bio-Rad 680 microplate reader, and analyzed with accompanying software Microplate Manager 5.2.

### 4.10. Quantitative real-time PCR

Total RNA of lung tissues was isolated by TRIzol Reagent (Invitrogen, Beijing, China), according to the manufacturer’s protocol. mRNA was reverse-transcribed using a Revert Aid First Stand cDNA Synthesis kit (Thermo Fisher, Beijing, China). Real-time PCR was performed using the SYBR Premix Ex Taq (Takara, Dalian, China). For MUC5AC gene, the primers used for qRT-PCR analysis are F: 5’-CAG CAT CAT CAA CAG CGA AAC-3’ and R: 5’-TAG TCA CAG AAC AGT GGG CAG A-3’. For  $\beta$ -actin gene, the primers used for qRT-PCR analysis are F: 5’-TGT GCC CAT CTA CGA GGG CTA T-3’ and R: 5’-TTT GAT GTC ACG CAC GAT TTC C-3’. The 2 $^{-\Delta\Delta Ct}$  method was used to calculate the relative expression. All PCR reactions were performed in triplicate.

#### 4.11. Western blot assay

Total protein of lung tissues was extracted using protein extraction kit (R0011; Solarbio Beijing). The concentration of total protein was detected by BCA kit (12002231, Bio-Rad, Hercules, CA, USA). The protein was separated by SDS-PAGE and transferred to PVDF membrane (Millipore, Shanghai, China). The membrane was blocked by non-fat milk and then incubated with primary antibodies for p-Akt (1:2000, 44-621G; Thermo Scientific), Akt (1:1000, MA5-14916; Thermo Scientific), and  $\beta$ -actin (1:10000, PA1-183; Thermo Scientific). After 12h of incubation at 4°C, the membrane was washed, incubated by the secondary antibody, and visualized by ECL (Millipore, MA, USA).  $\beta$ -actin serves as an internal control. Quantification of band densitometry was performed using ImageJ (NIH, Bethesda, MD, USA).

#### 4.12. Statistical analysis

Statistical analyses were performed using SPSS software (version 16.0; SPSS Inc., Chicago, IL, USA). Comparison between two groups or among multiple groups were analyzed by student t-test or one-way ANOVA, respectively. All data are expressed as the mean  $\pm$  standard deviation (SD) of at least three separate repeated experiments. Statistical significance was identified based on  $P < 0.05$ .

**Acknowledgement:** This work was supported by the Excellent youth program of Natural Science Foundation of Heilongjiang Province of China (No. YQ2019H011) and Innovation and Entrepreneurship Projects for College Students (202210226113).

**Authors' contribution:** Lixia Qiang and Qiang Li designed the study, conducted the experimental work, analyzed results and wrote the first draft of the manuscript. Qiang Li, Hang Shang, Guangrun Wu and Xiangshun Li participated in designing the study, experimental work, obtaining and analyzing the results. Qiang Li, Hang Shang, Xiangshun Li, Guangrun Wu and Lixia Qiang participated in drafting the article and critically revising it. All authors contributed to and have approved the final manuscript.

**Conflict of interest disclosure:** All authors have no financial interests or potential conflicts of interests to declare.

#### References

- Agustí A, Melén E, DeMeo DL, Breyer-Kohansal R, Faner R (2022) Pathogenesis of chronic obstructive pulmonary disease: understanding the contributions of gene-environment interactions across the lifespan. *Lancet Respiratory Medicine* 10: 512–524.
- Ahmad S, Mohd Noor N, Engku Nur Syafirah EAR, Irekeola AA, Shueb RH, Chan YY, Barnes PJ, Mohamad R (2023) Anti-tumor necrosis factor for supplementary management in severe asthma: a systematic review and meta-analysis. *J Interferon Cytokine Res* 43: 77–85.
- Barnes PJ (2016) Inflammatory mechanisms in patients with chronic obstructive pulmonary disease. *J Allergy Clin Immunol* 138: 16–27.
- Barnes PJ (2017) Cellular and molecular mechanisms of asthma and COPD. *Clin Sci (Lond)* 131: 1541–1558.
- Brunton B, Rogers K, Phillips EK, Brouillette RB, Bous R, Butler NS, Maury W (2019) TIM-1 serves as a receptor for Ebola virus in vivo, enhancing viremia and pathogenesis. *PLoS Negl Trop Dis* 13: e0006983.
- Busse PJ, Zhang TF, Schofield B, Kilaru S, Patil S, Li XM (2009) Decrease in airway mucous gene expression caused by treatment with anti-tumor necrosis factor  $\alpha$  in a murine model of allergic asthma. *Ann Allergy Asthma Immunol* 103: 295–303.
- Chae SC, Park YR, Song JH, Shim SC, Yoon KS, Chung HT (2005) The polymorphisms of Tim-1 promoter region are associated with rheumatoid arthritis in a Korean population. *Immunogenetics* 56: 696–701.
- Chen JP, Zhao WL, He NH, Gui Q, Xiong JP, Zhou HM, Wang Y, Chen S, Zhou P (2012) Association of Hepatitis A exposure and TIM-1 with childhood allergic asthma. *J Asthma* 49: 697–702.
- Curtiss ML, Gorman JV, Businga TR, Traver G, Singh M, Meyerholz DK, Kline JN, Murphy AJ, Valenzuela DM, Colgan JD, Rothman PB, Cassel SL (2012) Tim-1 regulates Th2 responses in an airway hypersensitivity model. *Eur J Immunol* 42: 651–661.
- Dang X, He B, Ning Q, Liu Y, Guo J, Niu G, Chen M (2020) Alantolactone suppresses inflammation, apoptosis and oxidative stress in cigarette smoke-induced human bronchial epithelial cells through activation of Nrf2/HO-1 and inhibition of the NF- $\kappa$ B pathways. *Respiratory Res* 21: 95.
- de Souza AJ, Oriss TB, O'malley KJ, Ray A, Kane LP (2005) T cell Ig and mucin 1 (TIM-1) is expressed on in vivo-activated T cells and provides a costimulatory signal for T cell activation. *Proc Natl Acad Sci U S A* 102: 17113–17118.
- Ding Q, Yeung M, Camirand G, Zeng Q, Akiba H, Yagita H, Chalasani G, Sayegh MH, Najafian N, Rothstein DM (2011) Regulatory B cells are identified by expression of TIM-1 and can be induced through TIM-1 ligation to promote tolerance in mice. *J Clin Invest* 121: 3645–3656.
- Feng BS, Chen X, He SH, Zheng PY, Foster J, Xing Z, Bienenstock J, Yang PC (2008) Disruption of T-cell immunoglobulin and mucin domain molecule (TIM)-1/TIM4 interaction as a therapeutic strategy in a dendritic cell-induced peanut allergy model. *J Allergy Clin Immunol* 122: 55–61. 61.e1–7.
- Fukushima A, Sumi T, Fukuda K, Kumagai N, Nishida T, Akiba H, Okumura K, Yagita H, Ueno H (2007) Antibodies to T-cell Ig and mucin domain-containing proteins (Tim)-1 and -3 suppress the induction and progression of murine allergic conjunctivitis. *Biochem Biophys Res Commun* 353: 211–216.
- Guan R, Wang J, Li D, Li Z, Liu H, Ding M, Cai Z, Liang X, Yang Q, Long Z, Chen L, Liu W, Sun D, Yao H, Lu W (2020) Hydrogen sulfide inhibits cigarette smoke-induced inflammation and injury in alveolar epithelial cells by suppressing PHD2/HIF-1 $\alpha$ /MAPK signaling pathway. *Int Immunopharmacology* 81: 105979.

- Gutor SS, Richmond BW, Du RH, Wu P, Lee JW, Ware LB, Shaver CM, Novitsky SV, Johnson JE, Newman JH, Rennard SI, Miller RF, Blackwell TS, Polosukhin VV (2022) Characterization of immunopathology and small airway remodeling in constrictive bronchiolitis. *Am J Respir Crit Care Med* 206: 260–270.
- Hosseini H, Yi L, Kanellakis P, Cao A, Tay C, Peter K, Bobik A, Toh BH, Kyaw T (2018) Anti-TIM-1 monoclonal antibody (RMT1-10) attenuates atherosclerosis by expanding IgM-producing B1a Cells. *J Am Heart Assoc* 7: e008447.
- Kaczka DW, Ingenito EP, Israel E, Lutchen KR (1999) Airway and lung tissue mechanics in asthma. Effects of albuterol. *Am J Respir Crit Care Med* 159: 169–178.
- Kersul AL, Iglesias A, Ríos Á, Noguera A, Forteza A, Serra E, Agustí A, Cosío BG (2011) Molecular mechanisms of inflammation during exacerbations of chronic obstructive pulmonary disease. *Arch Bronconeumol* 47: 176–183.
- Kim HY, Chang YJ, Chuang YT, Lee HH, Kasahara DI, Martin T, Hsu JT, Savage PB, Shore SA, Freeman GJ, Dekruyff RH, Umetsu DT (2013) T-cell immunoglobulin and mucin domain 1 deficiency eliminates airway hyperreactivity triggered by the recognition of airway cell death. *J Allergy Clin Immunol* 132: 414–425.e6.
- Kistemaker LE, Bos IS, Hylkema MN, Nawijn MC, Hiemstra PS, Wess J, Meurs H, Kerstjens HA, Gosens R (2013) Muscarinic receptor subtype-specific effects on cigarette smoke-induced inflammation in mice. *Eur Respir J* 42: 1677–1688.
- Li H, Li J, Lu T, Chen D, Xu R, Sun W, Luo X, Li H, Ma R, Wen W (2021) DZNeP attenuates allergic airway inflammation in an ovalbumin-induced murine model. *Mol Immunol* 131: 60–67.
- Li WX, Chen GM, Yuan H, Yao YS, Li RJ, Pan HF, Li XP, Xu JH, Tao JH, Ye DQ (2011) Polymorphisms of the TIM-1 and TIM-3 genes are not associated with systemic lupus erythematosus in a Chinese population. *Mutagenesis* 26: 507–511.
- Mannino DM, Buist AS (2007) Global burden of COPD: risk factors, prevalence, and future trends. *Lancet* 370: 765–773.
- Mariat C, Degauque N, Strom TB (2009) TIM-1: a new player in transplant immunity. *Transplantation* 87: S84–86.
- McIntire JJ, Umetsu DT, DeKruyff RH (2004) TIM-1, a novel allergy and asthma susceptibility gene. *Springer Semin Immunopathol* 25: 335–348.
- Meyers JH, Chakravarti S, Schlesinger D, Illes Z, Waldner H, Umetsu SE, Kenny J, Zheng XX, Umetsu DT, DeKruyff RH, Strom TB, Kuchroo VK (2005) TIM-4 is the ligand for TIM-1, and the TIM-1-TIM-4 interaction regulates T cell proliferation. *Nat Immunol* 6: 455–464.
- Miricescu D, Balan DG, Tulin A, Stiru O, Vacaroiu IA, Mihai DA, Popa CC, Papacocca RI, Enyedi M, Sorin NA, Vatachki G, Georgescu DE, Nica AE, Stefani C (2021) PI3K/AKT/mTOR signalling pathway involvement in renal cell carcinoma pathogenesis (Review). *Exp Ther Med* 21: 540.
- Niu J, Jiang Y, Xu H, Zhao C, Zhou G, Chen P, Cao R (2018) TIM-1 promotes Japanese encephalitis virus entry and infection. *Viruses* 10: 630.
- Nozaki Y, Nikolic-Paterson DJ, Yagita H, Akiba H, Holdsworth SR, Kitching AR (2011) Tim-1 promotes cisplatin nephrotoxicity. *Am J Physiol Renal Physiol* 301: F1098–1104.
- O'Byrne PM, Inman MD (2003) Airway hyperresponsiveness. *Chest* 123: 411S–416S.
- Pauwels NS, Bracke KR, Dupont LL, Van Pottelberge GR, Provoost S, Vanden Bergh T, Vandenabeele P, Lambrecht BN, Joos GF, Brusselle GG (2011) Role of IL-1 $\alpha$  and the Nlrp3/caspase-1/IL-1 $\beta$  axis in cigarette smoke-induced pulmonary inflammation and COPD. *Eur Resp J* 38: 1019–1028.
- Revathidevi S, Munirajan AK (2019) Akt in cancer: Mediator and more. *Sem Cancer Biol* 59: 80–91.
- Schweigert O, Dewitz C, Möller-Hackbarth K, Trad A, Garbers C, Rose-John S, Scheller J (2014) Soluble T cell immunoglobulin and mucin domain (TIM)-1 and -4 generated by a disintegrin and metalloprotease (ADAM)-10 and -17 bind to phosphatidylserine. *Biochim Biophys Acta* 1843: 275–287.
- Sharma G, Banerjee R, Srivastava S (2023) Molecular mechanisms and the interplay of important chronic obstructive pulmonary disease biomarkers reveals novel therapeutic targets. *ACS Omega* 8: 46376–46389.
- Sizing ID, Bailly V, McCoon P, Chang W, Rao S, Pablo L, Rennard R, Walsh M, Li Z, Zafari M, Dobles M, Tarilonte L, Miklasz S, Majeau G, Godbout K, Scott ML, Rennert PD (2007) Epitope-dependent effect of anti-murine TIM-1 monoclonal antibodies on T cell activity and lung immune responses. *J Immunol* 178: 2249–2261.
- Wang C, Xu J, Yang L, Xu Y, Zhang X, Bai C, Kang J, Ran P, Shen H, Wen F, Huang K, Yao W, Sun T, Shan G, Yang T, Lin Y, Wu S, Zhu J, Wang R, Shi Z, Zhao J, Ye X, Song Y, Wang Q, Zhou Y, Ding L, Yang T, Chen Y, Guo Y, Xiao F, Lu Y, Peng X, Zhang B, Xiao D, Chen CS, Wang Z, Zhang H, Bu X, Zhang X, An L, Zhang S, Cao Z, Zhan Q, Yang Y, Cao B, Dai H, Liang L, He J (2018) Prevalence and risk factors of chronic obstructive pulmonary disease in China (the China Pulmonary Health [CPH] study): a national cross-sectional study. *Lancet* 391: 1706–1717.
- Wang FW, Su QS, Li CQ (2023) Identification of cuproptosis-related asthma diagnostic genes by WGCNA analysis and machine learning. *J Asthma* 60: 2052–2063.
- Wang H, Yang T, Shen Y, Wan C, Li X, Li D, Liu Y, Wang T, Xu D, Wen F, Ying B (2016) Ghrelin inhibits interleukin-6 production induced by cigarette smoke extract in the bronchial epithelial cell via NF- $\kappa$ B Pathway. *Inflammation* 39: 190–198.
- Wu Y, Li Y, Wu B, Tan C, He X, Xu B, Yu G, Wang H (2018)  $\beta$ -Arrestin2 inhibits expression of inflammatory cytokines in BEAS-2B lung epithelial cells treated with cigarette smoke condensate via inhibition of autophagy. *Cell Physiol Biochem* 50: 1270–1285.
- Xiao S, Brooks CR, Sobel RA, Kuchroo VK (2015) Tim-1 is essential for induction and maintenance of IL-10 in regulatory B cells and their regulation of tissue inflammation. *J Immunol* 194: 1602–1608.
- Xiao S, Najafian N, Reddy J, Albin M, Zhu C, Jensen E, Imitola J, Korn T, Anderson AC, Zhang Z, Gutierrez C, Moll T, Sobel RA, Umetsu DT, Yagita H, Akiba H, Strom T, Sayegh MH, DeKruyff RH, Khoury SJ, Kuchroo VK (2007) Differential engagement of Tim-1 during activation can positively or negatively costimulate T cell expansion and effector function. *J Exp Med* 204: 1691–1702.

---

## ORIGINAL ARTICLES

- Xie X, Shi X, Chen P, Rao L (2017) Associations of TIM-1 genetic polymorphisms with asthma: a meta-analysis. *Lung* 195: 353–360.
- Yang RN, Wu XJ, Gounni AS, Xie JG (2023) Mucus hypersecretion in chronic obstructive pulmonary disease: From molecular mechanisms to treatment. *J Translat Int Med* 11: 312–315.
- Yang Y, Li X, An X, Zhang L, Li X, Wang L, Zhu G (2020) Continuous exposure of PM2.5 exacerbates ovalbumin-induced asthma in mouse lung via a JAK-STAT6 signaling pathway. *Adv Clin Exp Med* 29: 825–832.
- Yeung MY, Ding Q, Brooks CR, Xiao S, Workman CJ, Vignali DA, Ueno T, Padera RF, Kuchroo VK, Najafian N, Rothstein DM (2015) TIM-1 signaling is required for maintenance and induction of regulatory B cells. *Am J Transplant* 15: 942–953.